

# Raising the Resurrection plate from an unfolded-slab plate tectonic reconstruction of northwestern North America since early Cenozoic time

# Spencer Fuston† and Jonny Wu

University of Houston, Department of Earth and Atmospheric Sciences, 3507 Cullen Boulevard, Houston, Texas 77204-5008, USA

#### **ABSTRACT**

The configuration of mid-ocean ridges subducted below North America prior to Oligocene time is unconstrained by seafloor isochrons and has been primarily inferred from upper-plate geology, including neartrench magmatism. However, many tectonic models are permitted from these constraints. We present a fully kinematic, plate tectonic reconstruction of the NW Cordillera since 60 Ma built by structurally unfolding subducted slabs, imaged by mantle tomography, back to Earth's surface. We map in threedimensions the attached Alaska and Cascadia slabs, and a detached slab below western Yukon (Canada) at 400-600 km depth that we call the "Yukon Slab." Our restoration of these lower plates within a global plate model indicates the Alaska slab accounts for Pacific-Kula subduction since ca. 60 Ma below the Aleutian Islands whereas the Cascadia slab accounts for Farallon subduction since at least ca. 75 Ma below southern California, USA. However, intermediate areas show two reconstruction gaps that persist until 40 Ma. We show that these reconstruction gaps correlate spatiotemporally to published NW Cordillera near-trench magmatism, even considering possible terrane translation. We attribute these gaps to thermal erosion related to ridge subduction and model midocean ridges within these reconstruction gap mid-points. Our reconstructions show two coeval ridge-trench intersections that bound an additional "Resurrection"-like plate along the NW Cordillera prior to 40 Ma. In this model, the Yukon slab represents a thermally eroded remnant of the Resurrection plate.

Our reconstructions support a "northern option" Farallon ridge geometry and allow up to ~1200 km Chugach terrane translation since Paleocene time, providing a new "tomographic piercing point" for the Baja-British Columbia debate.

#### INTRODUCTION

Subduction of mid-ocean ridges is an important control on magmatic patterns, are geochemistry, uplift, and deformation along the North American Cordillera (Dickinson and Snyder, 1979; Thorkelson and Taylor, 1989; Severinghaus and Atwater, 1990; Sisson et al., 2003b; Thorkelson et al., 2011; Eddy et al., 2016). However, the seafloor magnetic anomalies that would constrain the pre-Oligocene configuration of these mid-ocean ridges (Farallon, Kula, Resurrection isochrons) have been almost entirely subducted, leading to many conflicting models regarding ridge number and geometry (Fig. 1) (Bradley et al., 2003). Possible ridge-trench intersections in these models have been inferred from preserved Pacific plate seafloor magnetic anomalies (Engebretson et al., 1985), near-trench magmatism (Bradley et al., 2003; Haeussler et al., 2003; Madsen et al., 2006), inboard magmatism (Breitsprecher et al., 2003; Cole et al., 2006; Ickert et al., 2009), and deformation (Eddy et al., 2016) (Fig. 1). Improved constraints on these ancient ridge-trench intersections is not only important for North American tectonics but also for reconstructing past geometries and kinematics of the partially subducted Kula and Farallon oceanic plates (i.e., "Big Kula" and "Big Farallon" of Figs. 1A and 1B). The Kula, Farallon, and other plates once formed part of the Panthalassa superocean during Pangea assembly and have proved extremely challenging to reconstruct (Li et al., 2019; Torsvik et al., 2019), resulting in a call for a better link between surface geology and the deep mantle (Pavlis et al., 2019). In addition, constraining the Paleocene to recent ridge-trench intersections in this region details the fragmentary demise of the Farallon plate, potentially illuminating the mechanism and frequency of oceanic plate fragmentation. In this paper, we address these topics by presenting a new, fully kinematic unfolded-slab plate tectonic reconstruction of the Paleocene to present NW Cordillera that constrains the positions of these cryptic mid-ocean ridges.

The most straightforward class of pre-Oligocene North American tectonic models involve a single end-member ridge-trench intersection below the Pacific Northwest (Engebretson et al., 1985), Alaska (Bradley et al., 2003) (Figs. 1A and 1B), northern Mexico (i.e., "Southern Option" of Fig. 1A) (Engebretson et al., 1985), or areas in between. These end-member models stem, in part, from coeval suites of near-trench magmatism present in Alaska (Sanak-Baranof belt) and the Pacific Northwest (see Table S2 in supplemental materials1). Mid-ocean ridge subduction is thought to induce melting in the normally amagmatic and refrigerated forearc regions (i.e., near-trench magmatism), producing a robust but not fully unique geologic indicator of ridge-trench intersection (Bradley et al., 2003; Haeussler et al., 2003; Sisson et al., 2003b). However, a single ridge-trench intersection below either Alaska or the Pacific Northwest (Figs. 1A and 1B) can account for only one of these magmatic suites.

Another class of plate model involves two coeval ridge-trench intersections, one to generate the Alaskan near-trench magmatism and another to generate the Pacific Northwest intrusions (Fig. 1C). These proposed mid-ocean ridges imply an additional, now-vanished "Resurrection" plate between the Farallon and Kula plates during early Cenozoic time (Haeussler

GSA Bulletin;

https://doi.org/10.1130/B35677.1; 7 figures; 1 supplemental file.

<sup>†</sup>spencerfuston@gmail.com.

<sup>&</sup>lt;sup>1</sup>Supplemental Material. Two fully kinematic plate reconstruction files with associated videos, two data tables, and six supporting figures. Please visit https://doi.org/10.1130/GSAB.S.12915482 to access the supplemental material, and contact editing@geosociety.org with any questions.

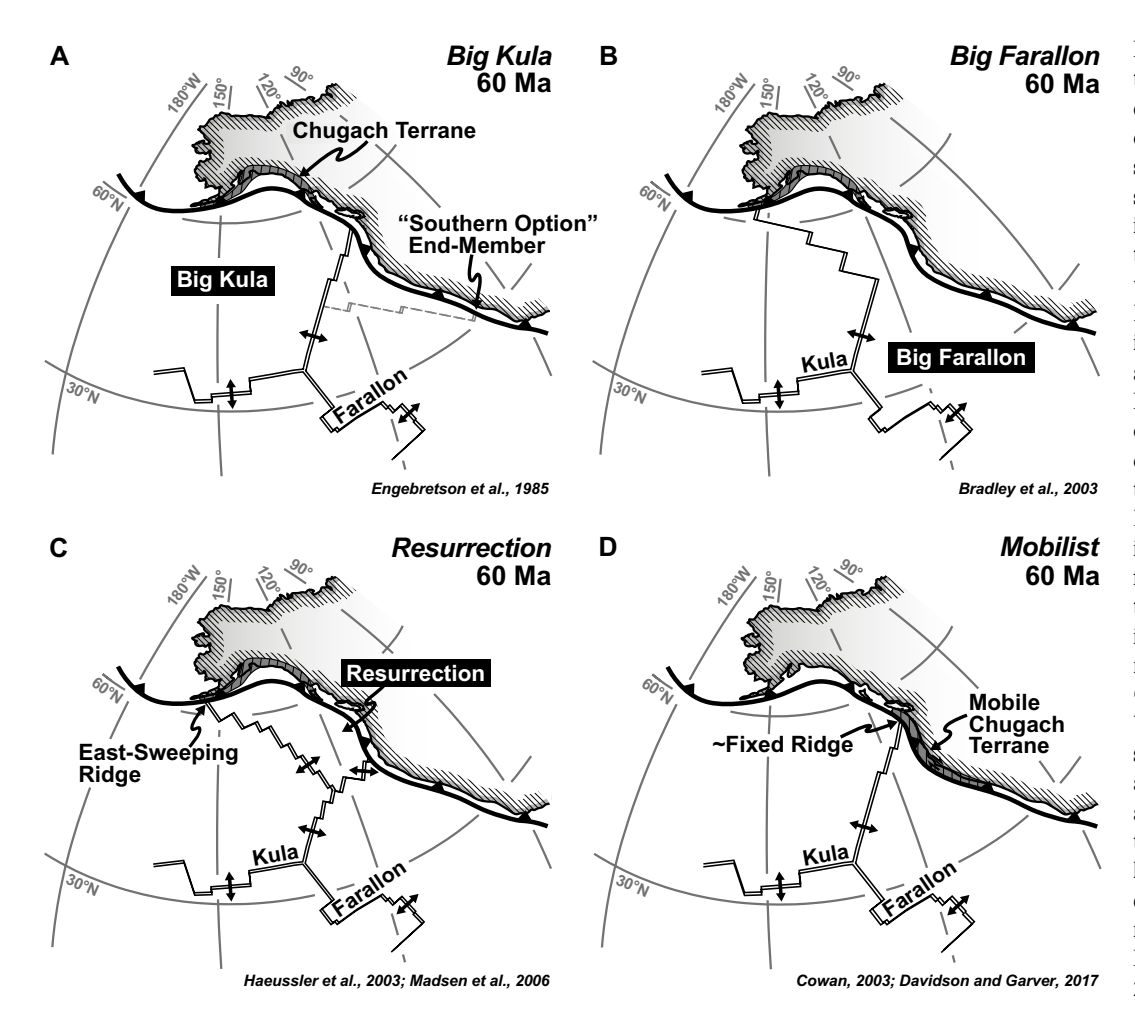


Figure 1. Published plate tectonic models of Paleocene western North America showing contrasting ridge-trench intersections. Models that invoke subduction of a single ridge imply (A) ridge-trench intersection below the Pacific Northwest and a comparatively larger Kula plate or (B) ridge-trench intersection along Alaska (USA) and a comparatively larger Farallon plate. In contrast, another model (C) invokes two coeval ridge-trench intersections bounding a now-vanished Resurrection plate. (D) "Mobilist" models attempt to account for near-trench magmatism through a single ridge-trench intersection and simultaneous northward translation of the Chugach terrane of Alaska. Variations of these models not shown here invoke intra-oceanic subduction offshore Alaska and/or the Pacific Northwest, thus precluding Kula or Farallon ridge-trench intersections during this period (e.g., Domeier et al., 2017; Sigloch and Mihalynuk, 2017; Vaes et al., 2019; Clennett et al., 2020).

et al., 2003; Madsen et al., 2006; Farris and Paterson, 2009; Scharman and Pavlis, 2012; McCrory and Wilson, 2013; Finzel and Ridgway, 2017). However, the Resurrection plate hypothesis has been questioned due to possible northward terrane translation along western North America (see below). Adding to this complexity are models that invoke back-arc basins offshore Alaska (Domeier et al., 2017; Vaes et al., 2019) or the entirety of western North America (Sigloch and Mihalynuk, 2017; Clennett et al., 2020) during early Cenozoic time (discussed below).

Paleomagnetic and geologic constraints place the Wrangellia composite terrane (WCT) and the Chugach accretionary complex (coastal British Columbia, Canada through southern Alaska) ~1000–3000 km to the south in Late Cretaceous time, indicating apparent northward terrane translation (Plumley et al., 1983; Coe et al., 1985; Bol et al., 1992; Stamatakos et al., 2001; Cowan, 2003; Wyld et al., 2006; Miller et al., 2006; O'Connell, 2009; Garver and Davidson, 2015). This has led to an alternative "Mobilist" plate tectonic model in

which a single Kula-Farallon spreading ridge was subducted below the contiguous United States, coeval with the northward translation of the overlying WCT (Cowan, 2003; Garver and Davidson, 2015) (Fig. 1D). This singular ridge subducts at an approximately stationary point below the northward moving terranes, producing the west to east younging of the Alaskan Sanak-Baranof belt (Fig. 1D). Some detrital zircon provenance studies have suggested these translated terranes were originally as far south as northern Mexico (Garver and Davidson, 2015; Day et al., 2016; Matthews et al., 2017). However, other correlations are possible because several permissible sediment sources exist along western North America (Surpless et al., 2014; Day et al., 2016; Matthews et al., 2017). Inboard magmatism (Breitsprecher et al., 2003; Thorkelson and Breitsprecher, 2005; Ickert et al., 2009) and deformation (Eddy et al., 2016) serve as corroborating evidence for ridge-trench intersection in the Pacific Northwest. Similar inboard evidence of ridge-trench intersection has been reported in Alaska (Cole et al., 2006). However, recent thermochronology data have been used to suggest a margin-parallel slab breakoff event instead (Terhune et al., 2019). If "Mobilist" models are correct, significant spatiotemporal uncertainty exists in interpreting upper plate geologic constraints for ridge-trench intersection models (Fig. 1).

Here we present the first fully kinematic, "Unfolded-Slab" plate tectonic reconstruction of western North America derived from structurally restoring subducted lithosphere back to Earth's surface (Fig. 2). Our aim is to reconcile conflicting tectonic models (Fig. 1) by reconstructing the subducted lower-plate from mantle tomography and testing our independently derived model against upper plate geology. Similar methods have been recently utilized for the South American Andes (Chen et al., 2019) and East Asia (Wu et al., 2016; Wu and Suppe, 2017). We discuss our results in the context of the presence of a Resurrection-like plate, northward terrane translation, the "Southern Option" Farallon ridgetrench intersection of Engebretson et al. (1985), preservation of subducted slabs, and Mesozoic North American tectonics.

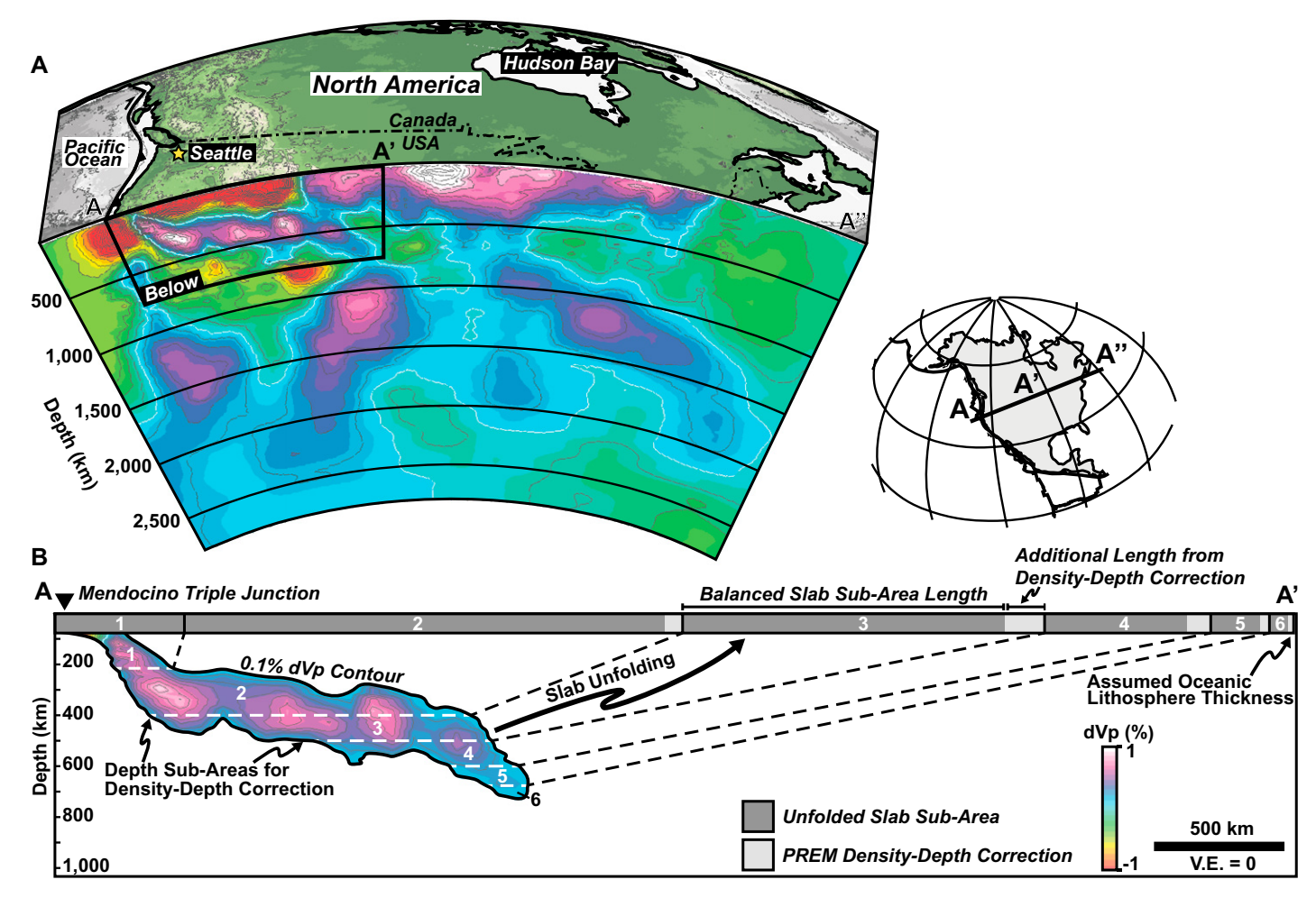


Figure 2. (A) Three-dimensional box diagram showing a tomographic cross-section of the North American mantle intersecting the Mendocino triple junction. Digital elevation topography is show at Earth's surface. (B) Tomographic transect A-A' from above showing an example of unfolding upper mantle subducted slabs back to Earth's surface. The picked Cascadia slab area is controlled by tomographic velocities (blue-purple colors). The gray bar at the top shows the unfolded slab length based on an assumed 80 km pre-subduction oceanic lithosphere thickness. A density-depth correction is applied along notated depth intervals following the Preliminary Reference Earth Model (PREM) (Dziewonski and Anderson, 1981). Tomography of Burdick et al. (2017). dVp—P-wave velocity perturbation; V.E.—vertical exaggeration.

#### **METHODS**

# **Slab Mapping from Tomography**

We identified potential subducted oceanic lithosphere below North America using recent ray-based and finite-frequency P-wave mantle tomography models (Amaru, 2007; Li et al., 2008; Sigloch, 2011; Schmandt and Lin, 2014; Burdick et al., 2017; Gou et al., 2019). Candidate slabs were mapped in three-dimensions from these tomographic models using the following criteria: faster-than-average (>0.2%) seismic P-wave velocity perturbation (dVp), Wadati-Benioff zone seismicity, slab-like geometry, continuity along strike, and consistency across all considered tomography models. We generated detailed three-dimensional mid-slab surface

maps for these candidate slabs following Wu et al. (2016), honoring earthquake hypocenters from a global catalog (Engdahl and Villasenor, 2002) (Fig. 3). Above 200 km depth, our mapped slab geometries were compared against the Slab2 model (Hayes et al., 2018) to mitigate degraded tomographic imaging at shallow depths.

#### **Slab Structural Restorations**

To quantify the amount of subducted oceanic lithosphere below North America we retrodeformed these slabs to their pre-subduction position at Earth's surface, following Wu et al. (2016). Our slab unfolding approach measures picked slab areas from spherical-Earth cross-sections and then restores a pre-subduction length of subducted lithosphere assuming a nominal slab thickness of 80 km (Fig. 2) (Richards et al., 2018). We guided our picked slab edges by closely spaced dVp contours that close around a slab anomaly, similar to previous studies (Wu et al., 2016; Chen et al., 2019). A density-depth correction following the Preliminary Reference Earth Model (PREM) (Dziewonski and Anderson, 1981) was applied to account for increased compression with depth in the mantle. This process was repeated for ten tomographic transects along strike (Figs. 3 and 4). Each transect was oriented along computed plate convergence paths (i.e., North American upper plate relative to a Kula or Farallon oceanic lower plate) following (Ren et al., 2007). Thus, our restored slab lengths define curved paths with plate tectonic significance rather than straight line approximations (see curved restored slab lengths shown

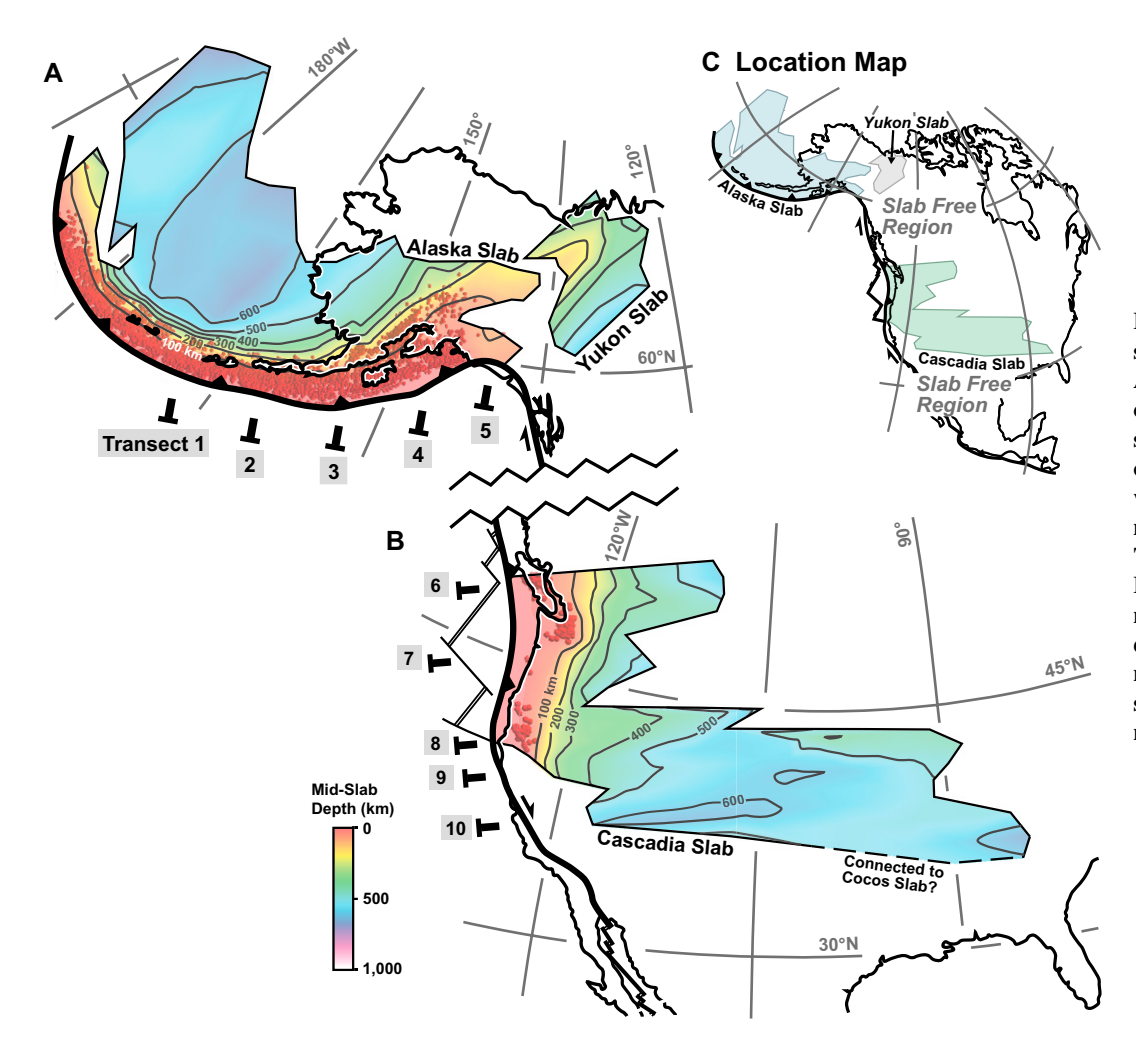


Figure 3. Mid-slab surface structure maps for the (A) Alaska, Yukon, and (B) Cascadia slabs. (C) Location map showing the overall locations of slabs and slab gaps along western North America. Seismicity shown by red points. Tomographic transect lines for Figure 4 are shown. The slab maps are composite maps produced from three-dimensional mapped surfaces from all considered mantle tomography models (see methods).

by the darker lines within the colored areas of Fig. 5).

## **Unfolded-Slab Plate Tectonic Modeling**

We built a quantitative, unfolded-slab plate tectonic model by placing our unfolded-slab results into a seafloor-spreading based global plate model (Matthews et al., 2016) using the software GPlates (Boyden et al., 2011). We developed a fully kinematic plate model by first assigning plate motions to our unfolded slab lengths that are attached to present-day subduction zones (i.e., attached slabs) and then imposing conjugate seafloor isochrons on our reconstructed seafloor (Matthews et al., 2016). The detached Yukon slab below western Yukon. Canada (discussed later) was modeled to be static within a mantle reference frame to produce a straightforward interpretation, and then incorporated into our final plate tectonic reconstruction by inspection as a suitable fit was discovered within a plate reconstruction "gap." To assess possible mantle reference uncertainty, we test

our unfolded-slab plate model against multiple mantle reference frames (Fig. S4; see footnote 1) (O'Neill et al., 2005; Torsvik et al., 2008; Torsvik et al., 2019).

#### RESULTS

Ten tomographic cross-sections from southern California to the Aleutian Islands were analyzed using the MITP16 (Burdick et al., 2017), MITP08 (Li et al., 2008), and UUP07 (Amaru, 2007) global P-wave tomography models. The S&L14 (Schmandt and Lin, 2014) P-wave and Sigloch11 (Sigloch, 2011) finite-frequency region-specific tomography models were also analyzed below the contiguous United States; the Gou19 (Gou et al., 2019) local P-wave tomography was analyzed below Alaska. Mean unfolded slab lengths were calculated to estimate the amount of subducted slab held within each tomographic transect. Below, we first present our Alaska and Cascadia slab mapping results, followed by our slab unfolding below these regions.

# Three-Dimensional Slab Mapping from Mantle Tomography

# Alaska Slab Mapping

For the purposes of our analysis, we define the Alaska slab as coherent slab-like highvelocity anomalies that connect upwards to the modern Aleutian-Alaskan subduction zone. We therefore exclude the voluminous lower mantle anomaly present at ~900 km depth below the modern Gulf of Alaska (Domeier et al., 2017; Vaes et al., 2019), labeled "Deep Alaska" in Figure S1 (see footnote 1 for all supplemental figures). Our Alaska slab mapping reveals a steeply dipping (>45°) upper mantle slab geometry below the Aleutian Islands eastward to the longitude of mainland Alaska (~160°W). At depth, this western Alaska slab rests horizontally across the uppermost lower mantle (~700 km depth) (Fig. 3A). This flat geometry is apparent in transects 1-3 across all considered tomography models (Figs. S1a-S11), except the Gou19 tomography which did not fully image the area in transect 1 (Fig.

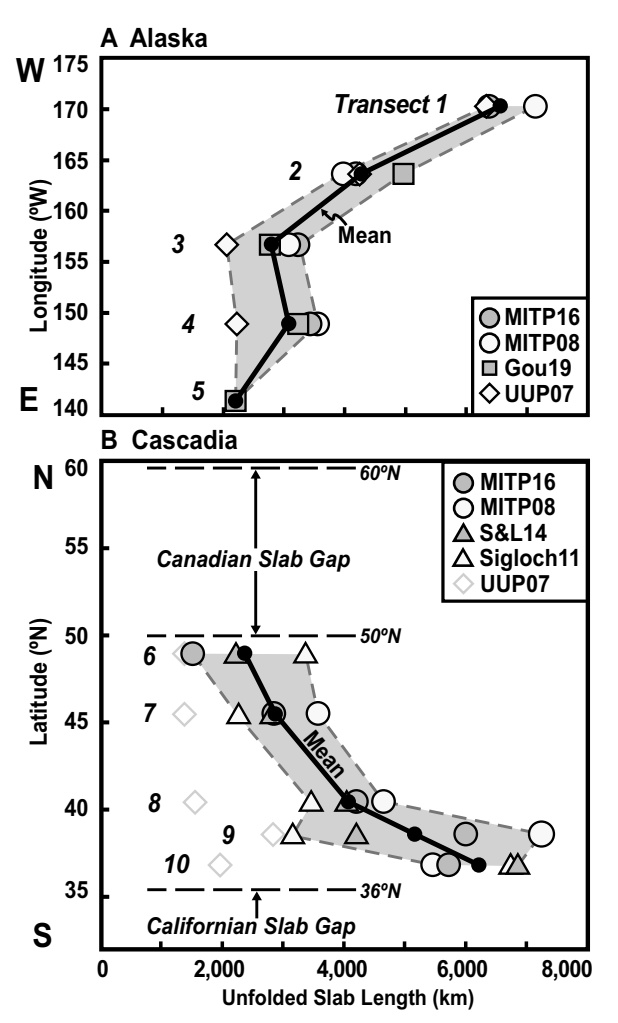


Figure 4. Unfolded pre-subduction slab lengths for the North American (A) Alaska and (B) Cascadia slabs. Transects 1-10 correspond to those of Figure 3. Black lines represent the statistical mean of slab unfolding results for each transect. Areas labeled "Canadian Slab Gap" and "Californian Slab Gap" mark areas between 50°N and 60°N latitude and south of 36°N latitude along western North America that do not show coherent subducted slab anomalies. Tomography models used for this analysis are: MITP16 (Burdick et al., 2017), MITP08 (Li et al., 2008), Gou19 (Gou et al., 2019), UUP07 (Amaru, 2007), S&L14 (Schmandt and Lin, 2014), and Sigloch11 (Sigloch, 2011). The UUP07 model showed systematically shorter Cascadia slab lengths and, based on our criteria, were not considered in our statistical mean values but are shown for completeness.

S1a). The horizontally oriented Alaska slab increases in aerial extent systematically westward to approximately ~165°E (Fig. 3A). East of Anchorage, Alaska, the slab becomes more shallowly dipping (Fig. 3A) in response to the presently colliding Yakutat terrane (Gutscher et al., 2000; Finzel et al., 2011). Transects 3–5 document this systematic shallowing of the Alaska slab in all considered tomography models (Figs. S1i–S1q). A margin-parallel slab tear is observed in this horizontally oriented slab in the tomography of Gou et al. (2019) (Fig. S1q). Sharp slab truncations are present along the eastern (~140°W) and northern limit of the Alaska slab (Fig. 3A).

We also mapped a less well-imaged, high-velocity anomaly below western Yukon at ~400–600 km depth, herein referred to as the "Yukon slab" (Fig. 3A). We differentiate our Yukon slab from the "Yukon anomaly," which is a deeper, unrelated tomographic feature from a previous study (van der Meer et al., 2018). This additional slab is better resolved by the recent local tomography of Gou et al.

(2019). The Yukon slab extends eastward to ~120°W and appears to be disconnected from the Alaska slab to the west in both local and global tomography models (Fig. 3A; Fig. S3). Additional, localized high-velocity anomalies are imaged farther south of the Yukon slab (Fig. S3). These anomalies may represent extensions of the Yukon slab, but were not considered here because they do not meet our interpretation criteria (i.e., non-continuous along strike and were only present at the outer resolution limits of the Gou19 tomography model). Nevertheless, we consider the possibility for a larger Yukon slab in our later discussion.

The shallow (<300 km depth) structure of our mapped Alaska slab generally agrees with previous studies (Hayes et al., 2018; Gou et al., 2019). However, we map an abrupt northern limit of the Alaska slab that does not connect to the adjacent Yukon slab, rather than a steeply dipping northern boundary as has been proposed previously (Jadamec and Billen, 2010; Gou et al., 2019). Below 300 km depth, few studies have attempted to map aseismic por-

tions of the Alaska slab; however, the horizontal geometry of the slab (Fig. 3A) is corroborated by all considered tomography models (Figs. S1b–S1h).

# Cascadia Slab Mapping

We only consider coherent slab-like anomalies that connect upwards to the modern Cascadia subduction zone to be Cascadia slab. The Cascadia slab extends from ~50°N to 37°N and our mapping (Fig. 3B) reveals that it is divided into two main segments: a northern, "shorter" segment (Figs. S2a-S2j) and a southern, "longer" segment (Figs. S2k-S2y). The transition between the two segments is at ~45°N (northern Oregon, USA) (Fig. 3B). The shorter, northern Cascadia slab segment extends eastward to ~110°W (below central Montana, USA), while the longer, southern segment reaches as far as ~84°W (below central Georgia, USA) (Fig. 3B). This latitudinal variation in slab geometry is corroborated by all considered tomography models (Fig. S2). South of the Mendocino Triple Junction (~40°N), the Cascadia slab is disconnected from the modern subduction zone but connects laterally to adjacent slab (Fig. 3B; Figs. S2p–S2y). A sharp margin-perpendicular truncation below northern Vancouver Island marks the northern limit of the Cascadia slab (Fig. 3B). The southern limit is less well-imaged and appears to converge toward the Cocos slab subducted below Central America (Fig. 3B). Steeply dipping slab geometries below Idaho, USA have been previously interpreted as a stagnant slab connected upwards to North America (Figs. S2f and S2g) (Schmandt and Humphreys, 2011) or as a folded extension of the Cascadia slab (Sigloch and Mihalynuk, 2017) (Fig. S2j). We do not include this feature in our Cascadia slab map because its geometry varies between tomography models, and its spatial connection to the Cascadia slab is unclear (Figs. S2f-S2i). However, for completeness we include these possible slabs in our slab unfolding analysis (transect 7 of Figs. 3B and 4B), noting that these slabs only account for minor variation (21% difference; compare transect 7 minimum and mean values of Fig. 4) and thus do not change our interpretations.

Our Cascadia slab map is characterized by a northern "short" region and a southern "long" region (Fig. 3B) that broadly agrees with study predictions that invoke conjugate Shatsky Rise subduction as a control on Farallon slab geometries (Saleeby, 2003; Liu et al., 2010; Humphreys et al., 2015). The southern limit of our mapped Cascadia slab extends farther south and east than previously suggested (Pavlis et al., 2012) which has implications for the latitudes of our modeled ridge-trench intersections (e.g., Fig. 6).

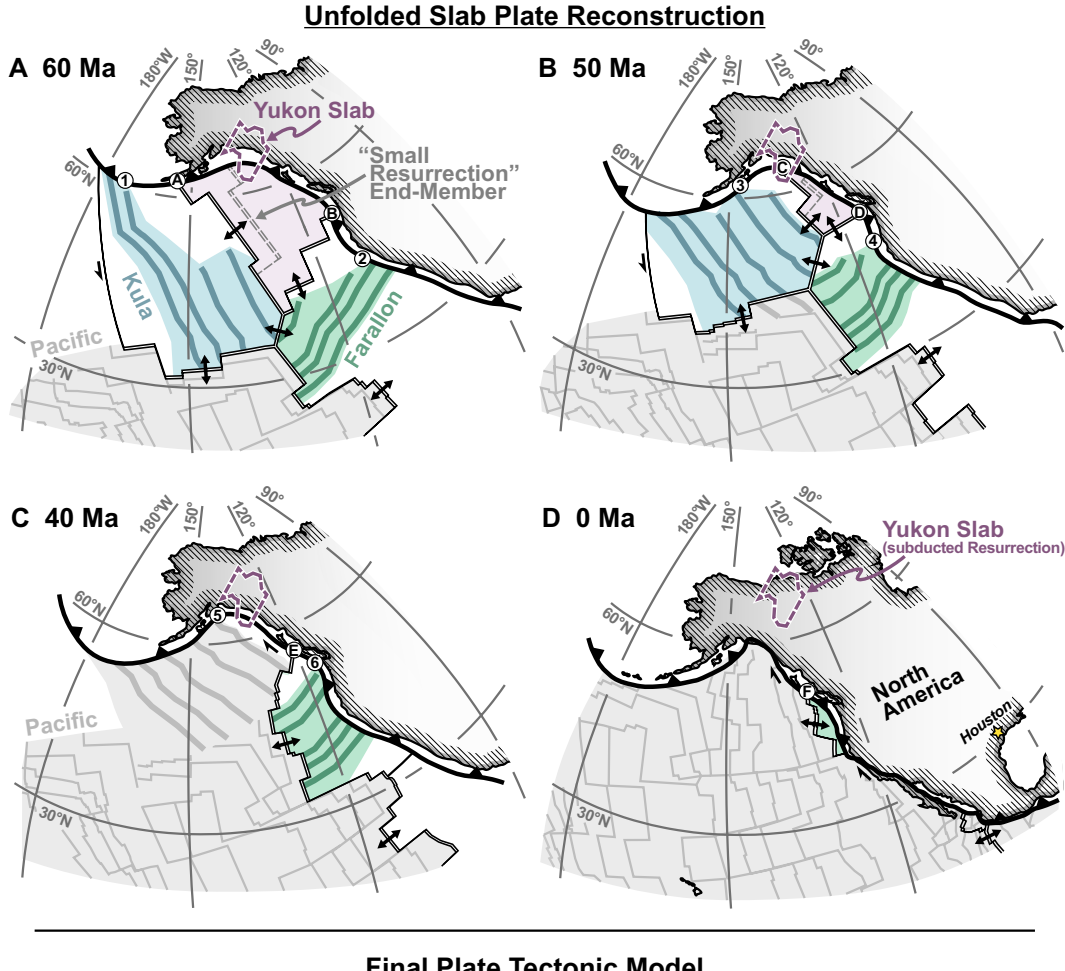
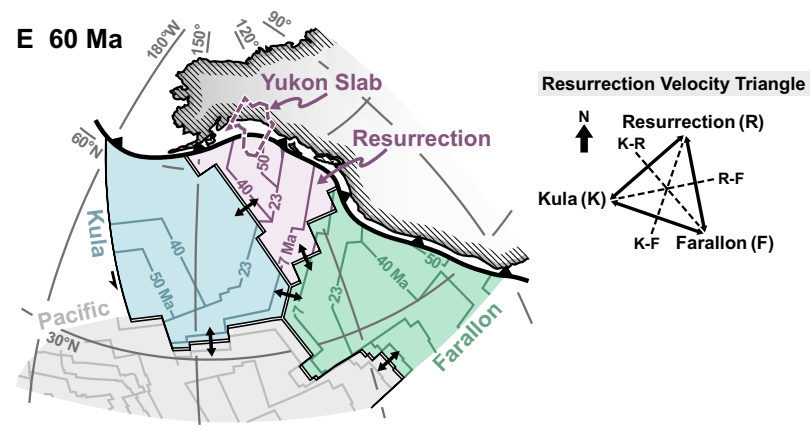


Figure 5. Unfolded-slab plate reconstruction tectonic western North America at (A) 60 Ma, (B) 50 Ma, (C) 40 Ma, and (D) present-day. Unfolded slab lengths from this study are shown by darker colored lines and associated colored regions. For reference, the final ridge geometries and Resurrection plate (purple area) for all time intervals from (E) are superimposed. Aerial extent of the Yukon slab shown by dashed black lines. (E) Final plate tectonic model at 60 Ma integrating our modeled ridge geometries from Figure 6, seafloor isochrons with ages at 60 Ma, and an assumed equalangle Resurrection-Kula-Farallon triple junction geometry (see plate velocity triangle to the right). See also the GPlates files and Plate Reconstruction Videos in supplemental materials.

# **Final Plate Tectonic Model**



#### Slab Area Unfolding

#### Alaska Slab

Slab area unfolding was applied to five transects across Alaska and the Aleutian Islands using the global P-wave tomography models: MITP16 (Burdick et al., 2017), MITP08 (Li et al., 2008), and UUP07 (Amaru, 2007), and Gou19 local P-wave tomography (Gou et al., 2019). Our Alaska slab unfolding reveals

mean pre-subduction slab lengths that broadly decrease from west to east, with western unfolding results on the order of  $6610 \pm 530$  km and eastern results of  $2550 \pm 550$  km (Fig. 4A; see Table S1; see footnote 1). At transect five, only the Gou19 tomography shows a coherent subducted slab and is thus the only measurement reported. We use the mean unfolded slab length from each transect (solid lines of Figs. 4 and 6) as an input to our plate tectonic reconstruction. However, we address variability in our unfolded slab lengths by also modeling a minimum and maximum slab length scenario (dashed lines of Figs. 4 and 6). These alternative cases similarly reveal a broadly decreasing eastward trend with variability on the order of ~5 m.y.

#### Cascadia Slab

Slab area unfolding was applied to five transects across the contiguous United States using

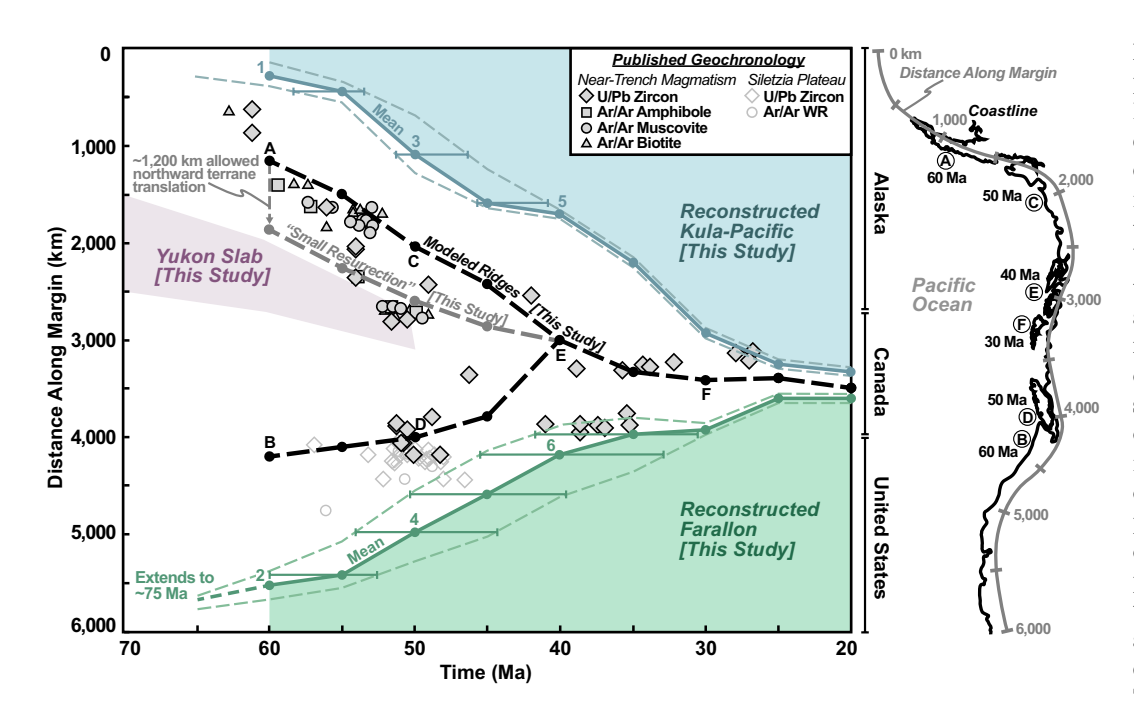


Figure 6. Spatiotemporal comparison of our reconstructed Kula-Pacific and Farallon subduction histories along western North America (colored regions) to published neartrench magmatism (gray symbols), plotted as distance along the North American margin against time. Distance along the margin is illustrated in the map on the right. Points 1-6 correspond to the circled numbers of Figure 5. Blue regions represent time accounted for by our reconstructed Kula-Pacific plates; green region represents reconstructed Farallon plate; purple region represents the present-day Yukon slab relative to the reconstructed western North American margin. The plate reconstruction gaps

(white regions) generally correlate to the published near-trench magmatism after 60 Ma. We attribute the gaps to thermal erosion related to ridge subduction. Therefore, we model ridge-trench intersections within the reconstruction gap mid-points (dashed black lines). Points A–F correspond to those of Figure 5. Near-trench magmatism references: Anderson and Reichenbach (1991); Bradley et al. (2000); Eddy et al. (2016); Haeussler et al. (1995); Madsen et al. (2006); Wells et al. (2014). WR—whole rock.

the same global P-wave tomography models as for the Alaska slab as well as the S&L14 local P-wave tomography (Schmandt and Lin, 2014) and the Sigloch11 local P-wave finite frequency tomography (Sigloch, 2011). Cascadia slab unfolding results reveal mean pre-subduction slab lengths that decrease systematically from south to north, ranging from  $6190 \pm 730 \text{ km}$ (south) to  $2370 \pm 990$  km (north) (Fig. 4B; see Table S1). The UUP07 tomography images the Cascadia slab as discontinuous, relatively slower-velocity anomalies, yielding unfolded slab lengths that are consistently shorter than all other considered tomography models (Fig. 4B). We, therefore, consider the UUP07 unfolding as minimum lengths and exclude them from our analysis. Minimum and maximum slab length cases are evaluated and determined to reinforce the south to north decrease in unfolded slab lengths, with variability on the order ~3-5 m.y. (dashed lines of Figs. 4 and 6).

# **Unfolded-Slab Plate Tectonic Modeling**

We reconstruct ancient Kula-Pacific and Farallon seafloor that has been lost to subduction by inputting our Alaska slab unfolding results into our selected global plate model (Fig. 5) (Matthews et al., 2016). Alternative mantle reference frames do not materially affect our slab reconstruction (Fig. S4) (O'Neill et al., 2005; Torsvik

et al., 2008; Torsvik et al., 2019). The westernmost Alaska slab lengths (blue shaded regions of Fig. 5) account for ca. 60 Ma of Pacific-Kula subduction below the Aleutian Islands whereas the southernmost Cascadia slab lengths (green shaded regions of Fig. 5) account for at least ca. 75 Ma of Farallon subduction below southern California (see supplemental GPlates files). The intermediate regions (i.e., between circled numbers 1 and 2 of Fig. 5A) are a plate reconstruction gap that is not accounted for by our lower-plate restorations. The present-day location of the Yukon slab (dashed black lines of Fig. 5) fits within this plate reconstruction gap and is mostly outboard of western North America. Moving forward in time, this plate reconstruction gap progressively closes from north and south between 50 Ma (circled numbers 3 and 4 of Fig. 5B) and 40 Ma (circled numbers 5 and 6 of Fig. 5C). During these times, the Yukon slab is also overridden by the westward-moving North American margin (Figs. 5B and 5C). For reference, we show our reconstructed Resurrection plate (purple shaded regions of Fig. 5) and final modeled spreading ridges within the reconstruction gap from 60 Ma to 40 Ma (Figs. 5A to 5C). These features are from our final plate model that integrates other constraints and assumptions into a fully kinematic, unfoldedslab plate model that we present in the Discussion section.

#### DISCUSSION

#### Comparison to Near-Trench Magmatism

Our unfolded slab-derived plate tectonic reconstruction (Figs. 5A to 5D) is built entirely from geophysical constraints and can be tested against relatively independent geologic observations. As previously mentioned, near-trench magmatism present in Alaska and the Pacific Northwest have been a key constraint for reconstructing western North American ridge-trench intersections (Bradley et al., 2003; Haeussler et al., 2003; Madsen et al., 2006). We compare this record of anomalous near-trench magmatism (gray symbols of Fig. 6; see Table S2) to our unfolded-slab plate reconstruction (colored area of Fig. 6). This is done by tracking the intersection points of our reconstructed Kula-Pacific, Farallon plates, and the Yukon slab with the western margin of North America (points 1-6 of Figs. 5 and 6). This analysis reveals that the intersection points of our reconstructed slabs with North America bound, but broadly do not overlap, the observed near-trench magmatism (points 1-6 of Figs. 5 and 6). Consequently, the unconstrained time between our three reconstructed slabs mirrors the trend observed in near-trench magmatism since Paleocene time (unshaded region of Fig. 6). This correlation implies that the mechanism which generated

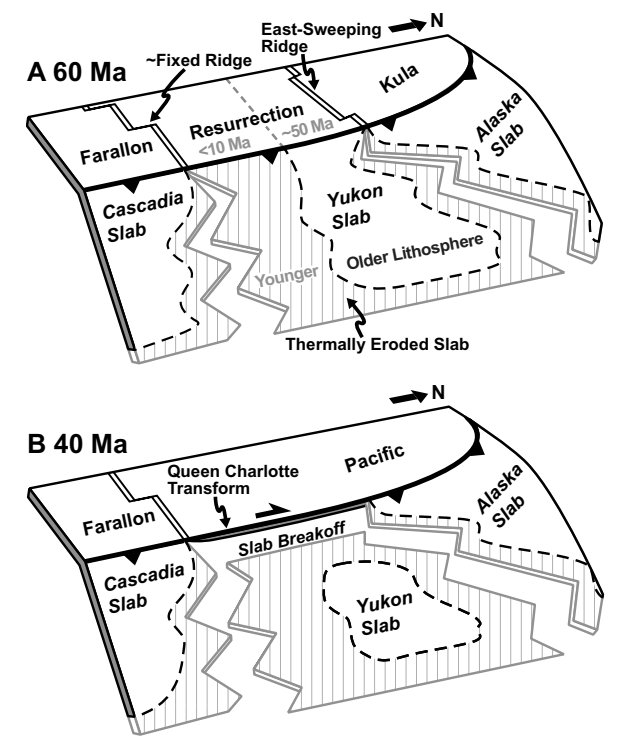


Figure 7. Cartoon of our interpreted history of Paleocene to recent slab windows below the North American Cordillera. (A) At 60 Ma, coeval subduction of two mid-ocean ridges (Farallon-Resurrection and Resurrection-Kula) produces two slab windows under the under the NW Cordillera astride the subducted Resurrection slabs (i.e., the "Yukon" slab in this study). Thermal erosion occurs along the slab window edges but is exaggerated on the southern half of the Resurrection slab due to very young lithospheric age (<10 Ma). (B) By 40 Ma, thermal erosion also occurs along the shallow Resurrection slab due to slab breakoff. This amplifies the thermal erosion and results in a smaller present-day Yukon slab anomaly. The dextral Queen Charlotte transform is active along the Canadian margin after 40 Ma.

the near-trench magmatism also controlled the selective preservation of subducted lithosphere. We acknowledge that <sup>40</sup>Ar/<sup>39</sup>Ar amphibole, muscovite, and biotite data may represent cooling ages. We include these data for completeness and note that these data show an overall trend that is broadly similar to that of available U-Pb zircon/ monazite ages. Alternative minimum and maximum slab length cases (dashed lines of Figs. 4 and 6) and mantle reference frames (Fig. S4) do not materially change this correlation.

Correlation between our unfolded-slab plate reconstruction gaps and the relatively independent near-trench magmatism is unlikely to be coincidental. Rather, we interpret these reconstruction gaps to be related to subduction of young, warm lithosphere near a midocean ridge. In this case, thermal erosion and melting of slab window fringes during ridge subduction would be expected (Dickinson and Snyder, 1979; Severinghaus and Atwater, 1990; Thorkelson and Breitsprecher, 2005; Thorkelson et al., 2011). Subducted young oceanic lithosphere would also become less visible or fully invisible to mantle tomography because upper mantle seismic velocities are primarily affected by temperature; composition, partial melting, anelasticity, and anisotropy play lesser roles (Goes et al., 1997). Indeed, kinematic thermal models of the subducted Farallon slab below western North America imply slower-velocity

to near-invisible slab regions should exist due to lithospheric thermal variations related to ridge subduction (Schmid et al., 2002). Modern-day analogues such as the actively subducting Chile Rise show a slower-velocity "slab window" due to ridge-trench intersection (Russo et al., 2010). Additionally, mantle convection models and seismic tomography indicate that gaps in subducted slabs due to ridge-trench intersection persist in the mantle over significant geologic time (at least 80 Ma) (Bunge and Grand, 2000). Therefore, we link our reconstructed "gap" and correlated near-trench magmatism to slab thermal erosion (hachured areas of Fig. 7) related to mid-ocean ridge subduction.

Accordingly, we model two mid-ocean ridges (i.e., the Kula-Resurrection and Resurrection-Farallon ridges) within the mid-points of the reconstruction gaps between our restored Kula-Pacific, Farallon, and Yukon slabs (dashed black lines of Fig. 6). These modeled ridge-trench intersection points along the NW Cordillera show a reasonable fit to observed near-trench magmatism (points A-F in Fig. 5). In this interpretation, the Yukon slab fits as a thermally eroded fragment of the subducted Resurrection plate (Fig. 7). However, a significant portion of magmatism in the Pacific Northwest has been attributed to the Siletzia oceanic plateau, erupted as the Farallon mid-ocean ridge passed over the Yellowstone hotspot (Wells et al., 2014; Eddy et al., 2016, 2017). We note that, in this interpretation, Siletzia magmatism still records the position of the Farallon-Resurrection ridge and consider it a useful constraint. A hotspot origin for the Siletzia plateau is compatible with our unfolded-slab results.

The general correlation between our unfoldedslab reconstruction and observed near-trench magmatism (Fig. 6) implies two coeval ridgetrench intersections that induced melting in both the normally-refrigerated forearc region (i.e., near-trench intrusions) (Bradley et al., 2003; Haeussler et al., 2003; Sisson et al., 2003a) and along the fridges of slab windows as fraternal slabs diverge after subduction (Dickinson and Snyder, 1979; Thorkelson and Taylor, 1989; Severinghaus and Atwater, 1990; Thorkelson, 1996; Atwater and Stock, 1998; Thorkelson and Breitsprecher, 2005; Thorkelson et al., 2011). These two mid-ocean ridges imply an additional tectonic plate between the Kula and Farallon plates offshore western North America during early Cenozoic time (purple shaded region of Fig. 5). Previous studies have proposed vanished plates along the NW Cordillera in early Cenozoic time (Fig. 1C) (Haeussler et al., 2003; Madsen et al., 2006). Here we adopt the name "Resurrection" for our reconstructed additional plate due to the similarity (in timing and origin) to this class of plate model (Fig. 1C).

# A Fully Kinematic Unfolded-Slab Plate Tectonic Reconstruction of the NW Cordillera since Early Cenozoic

We aim to further test our plate model plausibility by integrating the following elements into a fully kinematic plate tectonic reconstruction (example shown in Fig. 5E): (1) our unfoldedslab results (Figs. 5A-5D), (2) our modeled ridge-trench intersection points (points A-F in Figs. 5 and 6), and (3) Kula-Pacific synthetic seafloor isochrons following Matthews et al. (2016). This "final plate model" is shown in Figure 5E (see also the Preferred Plate Reconstruction Video and GPlates files in supplemental materials). To reconstruct the kinematics of the wholly subducted Resurrection plate, we assume a straightforward equal-angle Farallon-Resurrection-Kula triple junction configuration (see plate velocity triangle of Fig. 5E). Thus, our modeled Resurrection plate velocities mirror those of the adjacent Kula-Farallon ridge (constrained by seafloor isochrons). These plate velocities are combined with our modeled ridgetrench intersection points (points A-F of Figs. 5 and 6) to constrain Kula-Resurrection and Resurrection-Farallon ridge geometries (Figs. 5A-5C). While we show the most straightforward kinematics for this unconstrained triple junction, any realistic angle between these modeled ridges could also satisfy the input conditions described above. Our reconstruction is based on the mantle reference frame of Torsvik et al. (2019) for the Pacific-Panthalassa realm, however, other reference frames yield similar conclusions (Fig. S4). Our modeled half-spreading rates for these unconstrained mid-ocean ridges reaches a maximum of 7.8 cm yr<sup>-1</sup> (between ca. 56 to 48 Ma) and are consistent with global plate velocities (Zahirovic et al., 2015).

#### Late Cretaceous to Early Eocene

Fragmentation of the Farallon plate at ca. 85 Ma yielded the rapidly spreading Kula plate (Woods and Davies, 1982). Our slab unfolding results indicate the Kula plate underwent additional fragmentation no later than 60 Ma, yielding the Resurrection plate and associated midocean ridges (Fig. 5E). The western limit of our reconstructed Kula plate is modeled as a northsouth trending transform because the Alaska slab does not appear to be present farther west of this point based on our slab mapping and unfolding (Figs. 3A and 5A). Kula-Resurrection ridgetrench intersection began to generate the Sanak-Baranof near-trench magmatism in Alaska at ca. 60 Ma (Fig. 6). Shortly after, Pacific Northwest near-trench magmatism began around 58 Ma due to Farallon-Resurrection ridge-trench intersection. Subduction of the Resurrection plate produced the Yukon slab (dashed black line of Fig. 5E), which is the only candidate slab present in the modern-day upper mantle below this region (Fig. S3). It is noteworthy that the Yukon slab is present only below the western half of our reconstructed Resurrection plate (Fig. 5A). The apparent lack of Yukon slab to the south is consistent with our reconstructed Resurrection plate ages (synthetic isochron lines of Fig. 5E). At 60 Ma, the subducting eastern half of the Resurrection plate is very young (<10 m.y.) whereas the western half of the plate is much older (50–55 m.y.) (Fig. 5E). These lithospheric ages are inherited directly from Kula and Farallon seafloor magnetic anomalies on the modern-day Pacific plate (Engebretson et al., 1985; Matthews et al., 2016). Therefore, it is possible that the high-velocity anomalies of the Yukon slab represent the preservation of only the oldest Resurrection lithosphere within the northwest half of the Resurrection plate (Fig. 7). The significantly younger and warmer southern half of the Resurrection plate would be more susceptible to thermal erosion and, thus, may now be melted, assimilated in the mantle, or invisible to tomography.

#### Early Eocene to Present-Day

In early Eocene time, the Resurrection plate continues to subduct below western Canada,

accompanied by the eastward migration of the Kula-Resurrection ridge-trench intersection (point C of Fig. 5B). The Resurrection-Farallon ridge-trench intersection migrates slightly northward (point D of Fig. 5B). At 50 Ma, the present-day Yukon slab is located directly below the western North American margin (Fig. 5B), which would fit our plate reconstruction assuming near-vertical slab sinking. By 40 Ma it is fully overridden (Fig. 5C), requiring that the Yukon slab is wholly subducted by this time (Fig. 6C). Breakoff of the Resurrection plate at ca. 40 Ma corresponds with the initiation of the Queen Charlotte transform along British Columbia and Alaska (Figs. 5C and 7B), in agreement with previous studies (Haeussler et al., 2003; Madsen et al., 2006; ten Brink et al., 2018). After 40 Ma, our plate reconstructions broadly agree with global plate reconstructions (Fig. 5D; see plate reconstruction video) (Matthews et al., 2016).

## Comparison to Published NW Cordillera Plate Tectonic Reconstructions

Our plate tectonic reconstructions are broadly compatible with published models that infer a Resurrection plate from upper plate geology alone (Haeussler et al., 2003; Madsen et al., 2006). However, Madsen et al. (2006) outlines a more complex history of ridge-trench intersection involving additional fragmentation of the Resurrection (three events) and Farallon (one event) plates based on interpretation of near-trench magmatism, including a significant amount of K-Ar age data (Fig. S6). The complex ridge-trench intersections proposed by Madsen et al. (2006) generally fit within the unconstrained areas (white areas of Fig. 6) between our restored oceanic lithosphere (colored areas of Fig. 6) but crosscut our tomographic constraints in certain areas (Fig. S6), indicating areas for re-evaluation. For example, the "Eshamy" plate of Madsen et al. (2006) represents an alternative interpretation for the Yukon slab involving additional fragmentation of the Resurrection plate ("Resurrection Fragmentation 2" of Fig. S6) but crosscuts our restored Kula-Pacific plate. Here we do not adopt the name "Eshamy" in our plate reconstruction because Madsen et al. (2006) predict the "Eshamy" plate was fully subducted by ca. 27 Ma, whereas our reconstruction shows the Yukon slab would have been overridden by (i.e., subducted beneath) North America much earlier, by ca. 50 Ma, based on its present position (Fig. 5B; see Fig. S6 for comparison). Nevertheless, the relative compatibility of Madsen et al. (2006) with our constraints indicates that additional plate model complexities are possible within our uncertainties and should be further investigated.

Previous workers have interpreted a lower mantle high-velocity anomaly present at 800-1500 km depth below the modern Gulf of Alaska (labeled "Deep Alaska" in Fig. S1) as evidence of a Cretaceous intra-oceanic subduction zone offshore Alaska (Domeier et al., 2017: Sigloch and Mihalynuk, 2017; Vaes et al., 2019; Clennett et al., 2020). This outboard subduction zone, however, would preclude the Kula-Resurrection plates from intersecting the North American margin; instead, these ridges would be subducted offshore between 60 and 50 Ma. Our unfolded-slab reconstruction provides independent geophysical evidence that newly link North American near-trench magmatism with Kula-Resurrection and Resurrection-Farallon ridge-trench intersection along the North American plate (Figs. 5 and 6). This implies that these ridges did interact with an Andean-style continental margin by 60 Ma, presenting challenges to plate models that show intra-oceanic subduction offshore Alaska after ca. 60 Ma.

# Farallon-North America Ridge-Trench Intersections: Northern or Southern Option?

The latitude of Farallon-Resurrection ridgetrench intersection from Late Cretaceous to Oligocene time is unconstrained by seafloor isochrons, thus two end-members have been previously proposed (Fig. 1A) (Engebretson et al., 1985): (1) a "northern option" that places the ridge-trench intersection along the Pacific Northwest and (2) a "southern option" that places the intersection along Mexico. Our accounting of lost Farallon lithosphere constrains the northwestern limit of the Farallon plate and thus implies a position for this cryptic triple junction that is most consistent with the "northern option" (Fig. 5E). In contrast, the "southern option" of Engebretson et al. (1985) implies a mid-ocean ridge configuration that would crosscut our restored Farallon plate (compare "southern option" case of Fig. 1A to Fig. 5A). Our Cascadia slab reconstruction (Figs. 4 and 6; see GPlates files in supplemental materials) constrains Farallon subduction along western North America since at least ca. 75 Ma. We acknowledge that that the Cascadia slab leading edge is challenging to delineate (e.g., Schmandt and Lin, 2014) and requires further analysis. Nevertheless, our results exclude a Farallon ridge-trench intersection along Mexico after 60 Ma, and probably since at least ca. 75 Ma. We cannot exclude a scenario involving an ephemeral Farallon ridgetrench intersection along northern Mexico prior to ca. 75 Ma that migrated rapidly northwards due to ridge jumps or specific ridge-transform geometries (e.g., Thorkelson and Taylor, 1989). Instead, our model most clearly implies this triple-junction likely resides north of Mexico, at the latitudes of the Pacific Northwest at 60 Ma and probably since ca. 75 Ma (Fig. 5E).

The apparent incompatibility of our results with the Farallon ridge located along Mexico since at least ca. 75 Ma has important implications for northward terrane translation models (i.e., Baja-British Columbia). The "southern option" ridgetrench intersection has been a preferred causal mechanism for the northward translation of the Baja-BC block (Umhoefer, 2003; Wyld et al., 2006). This is because a Farallon spreading ridge located farther south during the Late Cretaceous would produce northward plate motions along a significantly longer swath of western North America that would aid in northward terrane translation (Engebretson et al., 1985; Umhoefer, 2003; Wyld et al., 2006; Gehrels et al., 2009; Matthews et al., 2016). In contrast, our results indicate a relatively northern position for the Farallon ridge-trench intersection (Fig. 5E) that would still allow moderate Baja-BC northward translations (see discussion below) but would be unlikely to assist in terrane translation from much farther south (i.e., Mexico) after at least ca. 75 Ma.

# End-Member Northward Terrane Translation along Western North America

One crucial objection to Resurrection plate models is based on the proposed northward movement of the Chugach terrane during Sanak-Baranof belt emplacement (Cowan et al., 1997; Cowan, 2003; Garver and Davidson, 2015). A southern location of the Chugach terrane during this time would require either: (1) a Kula-Resurrection ridge located farther to the south or (2) emplacement of the near-trench intrusions by a single Kula-Farallon ridge subducting below the Pacific Northwest during northward translation of the Chugach terrane (Fig. 1D) (Cowan, 2003; Davidson and Garver, 2017). Although our method does not directly constrain Chugach terrane paleo-latitudes, our restored Farallon, Kula, and Yukon slabs correlate with observed NW Cordilleran near-trench magmatism in a straightforward fashion (i.e., without invoking terrane translations) (Fig. 6). This scenario is the most straightforward conclusion from our slab-unfolding results and thus our preferred model. However, our results allow a second possible model involving a more southern location for the Kula-Resurrection ridge-trench intersection, combined with ~1200 km of northward Chugach terrane translation (maximum translation allowed by our results) since 60 Ma; we call this the "Small Resurrection" alternative model (Figs. 5 and 6). We provide a fully kinematic model of this alternative terrane translation scenario (see "Small Resurrection" alternative plate reconstruction video and GPlates files in supplemental materials).

The Small Resurrection alternative model maintains the Kula-Resurrection ridge-trench intersection north of our reconstructed Yukon slab, thus preserving the link between the Kula-Resurrection ridge and Sanak-Baranof magmatism. This results in a maximum allowed Chugach terrane translation of ~1200 km since 60 Ma (Fig. 6; Fig. S5a), which is consistent with geologic estimates of translation along known faults (Wyld et al., 2006). For comparison, we perform a first-order rigid block restoration of the Chugach terrane and associated near-trench magmatism using the parameters outlined above and find a relatively good fit in terms of overall location along the margin and southward-migrating trend (Fig. S5a). For clarity, our unfolded-slab constraints require the Chugach terrane to reside within ~1200 km of its present-day location by 60 Ma but allow for the possibility of larger-scale terrane translation prior to that time. Thus, by constraining ridgetrench intersections from reconstructing the lower plate from subducted oceanic lithosphere, our results present a new "tomographic piercing point" for the Baja-BC debate that supports a "Northern Option" Farallon ridge geometry and a maximum of ~1200 km of northward Chugach terrane translation since 60 Ma.

Some "Mobilist" models involve a single, southern Kula-Farallon ridge-trench intersection along the Pacific Northwest, emplacing Sanak-Baranof near-trench magmatism as the overlying Chugach terrane migrates to the north (Fig. 1D). Comparison of the "Mobilist" model to our slab-unfolding results (Fig. S5b) reveal inconsistencies with the apparent plate reconstruction gap present between the Alaska and Yukon slabs (Figs. 3 and 6; Fig. S5b). We regard this gap as an important constraint as it is present in all considered local and global tomography models that image the Yukon slab (Fig. S3). In addition, we note models that require terrane translations since 60 Ma that are significantly greater than estimates based on known strikeslip faults may result in the Chugach terrane shielding near-trench magmatism in the Pacific Northwest from the Kula-Farallon ridge-trench intersection (i.e., insulated from the margin by the Chugach terrane and thus not in a forearc position). These models tend to require unreasonably rapid terrane translation rates (~40 cm yr<sup>-1</sup> calculated from Cowan (2003) between 61 and 59 Ma) that are significantly greater than global plate velocities (Zahirovic et al., 2015). For these reasons, we consider extreme "Mobilist" models inconsistent with our slab-unfolding results and acknowledge the apparent gap between the Alaska and Yukon slabs as a critical point in this debate that may be clarified by future tomographic imaging studies.

#### Preservation of Subducted Slabs

Thermal erosion or melting of oceanic lithosphere subducted on the fringes of slab windows is a key feature of ridge subduction (Severinghaus and Atwater, 1990; Thorkelson, 1996; Thorkelson and Breitsprecher, 2005; Thorkelson et al., 2011). The degree to which thermal erosion expands slab windows at the expense of the subducted slabs, however, is poorly understood. Degradation of subducted slabs is of particular interest in the North American Cordillera because a large amount of subduction is predicted below southeast Alaska and Canada while few high-velocity anomalies have been imaged below this region (Fig. 3). This discrepancy persists regardless of which mid-ocean ridge configuration is considered (Fig. 1), because all proposed models require a large degree of subduction below Canada.

Our unfolded-slab plate tectonic reconstructions provide independent constraints on the presence and position of the Kula-Resurrection and Resurrection-Farallon mid-ocean ridges, respectively. As such, our reconstruction provides a predicted amount of oceanic lithosphere that can be compared with the amount that can be recovered from mantle tomography. At 60 Ma, we calculate that ~33% (~2,300,000 km<sup>2</sup>) of the predicted Kula plate surface area and ~25% (~809,000 km<sup>2</sup>) of the Farallon plate is apparently missing based on a comparison of predicted and recovered slab areas (Fig. 5A). While it is not clear whether the missing Kula and Farallon slabs are due to tomographic imaging, slab melting, assimilation into the mantle, or other effects, we note the magmatic budget below slab windows is poorly understood. As such, our analysis provides a first-order, maximum estimate on the possible degree of slab melting. We provide these estimates to lay the groundwork for further research, since it is reasonable to expect that higher-fidelity tomographic imaging will become available throughout the North American Cordillera in the future.

# **CONCLUSIONS**

The orientation and number of mid-ocean ridges subducted below North America prior to Oligocene time has been obscured by subduction. We aim to recover these lost plate configurations by reconstructing the Kula, Farallon, and Resurrection lower plates as imaged by mantle tomography. We present a fully kinematic plate tectonic reconstruction of the Paleocene to recent North American Cordillera constrained

from structurally unfolding subducted slabs back to Earth's surface (Figs. 2 and 5), and an alternative model that includes limited ~1200 km northward terrane translation. Detailed threedimensional mid-slab mapping reveals that both the Alaska and Cascadia slabs rest horizontally across the uppermost lower mantle and decrease in aerial extent inwards toward British Columbia (Fig. 3). We also mapped localized high-velocity anomalies below western Yukon at ~400-600 km depth, referred to as the Yukon slab (Fig. 3A). Our slab unfolding analysis accounts for ca. 60 Ma of Kula-Pacific subduction time below western Alaska and at least ca. 75 Ma of Farallon subduction below southern California (Figs. 5A and 6). Intermediate regions under British Columbia show plate reconstruction gaps that persist until 40 Ma (unshaded regions of Fig. 6). We show that these reconstruction gaps correlate spatiotemporally to published NW Cordilleran near-trench magmatism since ca. 60 Ma and attribute the gaps to thermal erosion related to ridge subduction. We suggest that the subduction of two mid-ocean ridges bounding a "Resurrection" plate can explain this apparent correlation. In this interpretation the detached Yukon slab fits as a severely thermally eroded remnant of the Resurrection plate. Our slab-unfolding results constrain a maximum ~1200 km of northward Chugach terrane translation since 60 Ma and is illustrated by our alternative "Small Resurrection" model. Our unfolded-slab reconstructions contribute new insights on NE Pacific-Panthalassa realm reconstructions by constraining past Kula and Farallon plate geometries back to the early Cenozoic, terrane translation along western North America, and serving as an example of linking surface geology to the deep mantle by reconstructing ancient ridge-trench intersections.

#### ACKNOWLEDGMENTS

Support for this work was provided by National Science Foundation Division of Earth Sciences Grant EAR-1848327. We thank Mike Eddy and an anonymous reviewer for improving this manuscript via their thorough, well-considered, and critical reviews. We thank Derek Thorkelson, Paul Umhoefer, Virginia Sisson, Lorenzo Colli, John Suppe, Hans-Peter Bunge, Bram Vaes, Steve Grand, Maurice Colpron, and our lab members Yi-An Lin, Yi-Wei Chen, and Jeremy Tsung-Jui Wu for discussion. We are grateful for workshops and scientific visit discussions hosted by the University of Houston Center for Tectonics and Tomography. Paradigm provided GOCAD educational software licenses through the Paradigm University Program.

#### REFERENCES CITED

- Amaru, M., 2007, Global travel time tomography with 3-D reference models [Ph.D. thesis]: Utrecht, Netherlands, Utrecht University, 174 p.
- Anderson, R.G., and Reichenbach, I., 1991, U-Pb and K-Ar framework for Middle to Late Jurassic (172–158 Ma) and Tertiary (45–27 Ma) plutons in Queen Charlotte

- Islands, British Columbia, *in* Woodsworth, G.J., ed., Evolution and Hydrocarbon Potential of the Queen Charlotte Basin, British Columbia: Geological Survey of Canada, Paper 90-10, p. 59–87.
- Atwater, T., and Stock, J., 1998, Pacific-North America plate tectonics of the Neogene southwestern United States: An update: International Geology Review, v. 40, no. 5, p. 375–402, https://doi.org/10.1080/00206819809465216.
- Bol, A.J., Coe, R.S., Grommé, C.S., and Hillhouse, J.W., 1992, Paleomagnetism of the Resurrection Peninsula, Alaska: Implications for the tectonics of southern Alaska and the Kula-Farallon Ridge: Journal of Geophysical Research. Solid Earth, v. 97, p. 17213–17232, https:// doi.org/10.1029/92JB01292.
- Boyden, J.A., Müller, R.D., Gurnis, M., Torsvik, T.H., Clark, J.A., Turner, M., Ivey-Law, H., Watson, R.J., and Cannon, J.S., 2011, Next-generation plate-tectonic reconstructions using GPlates, in Keller, G.R., and Baru, C., eds., Geoinformatics: Cyberinfrastructure for the Solid Earth Sciences: Cambridge, UK, Cambridge University Press, p. 95–114.
- Bradley, D., Parrish, R., Clendenen, W., Lux, D., Layer, P., Heizler, M., and Donley, D., 2000, New geochronological evidence for the timing of early Tertiary ridge subduction in southern Alaska, in Kelley, K.D., and Gough, L.P., eds., Geologic Studies in Alaska by the U.S. Geological Survey, 1998: U.S. Geological Survey Professional Paper 1615, p. 5–21.
- Bradley, D.C., Kusky, T.M., Haeussler, P.J., Goldfarb, R.J., Miller, M.L., Dumoulin, J.A., Nelson, S.W., and Karl, S.M., 2003, Geologic signature of early Tertiary ridge subduction in Alaska, in Sisson, V.B., Roeske, S.M., and Pavlis, T.L., eds., Geology of a Transpressional Orogen Developed During Ridge-trench Interaction Along the North Pacific Margin: Geological Society of America Special Paper 371, p. 19–49, https://doi .org/10.1130/0-8137-2371-X.19.
- Breitsprecher, K., Thorkelson, D.J., Groome, W.G., and Dostal, J., 2003, Geochemical confirmation of the Kula-Farallon slab window beneath the Pacific Northwest in Eocene time: Geology, v. 31, no. 4, p. 351–354, https://doi.org/10.1130/0091-7613(2003)031<0351:GCOTKF >2.0.CO:2.
- Bunge, H.-P., and Grand, S.P., 2000, Mesozoic platemotion history below the northeast Pacific Ocean from seismic images of the subducted Farallon slab: Nature, v. 405, no. 6784, p. 337–340, https://doi .org/10.1038/35012586.
- Burdick, S., Vernon, F.L., Vladik, M., Eakins, J., Cox, T., Tytell, J., Mulder, T., White, M.C., Astiz, L., Pavlis, G.L., and van der Hilst, R.D., 2017, Model update May 2016: Upper-mantle heterogeneity beneath North America from travel-time tomography with global and US-Array data: Seismological Research Letters, v. 88, no. 2A, p. 319–325, https://doi.org/10.1785/0220160186.
- Chen, Y.-W., Wu, J., and Suppe, J., 2019, Southward propagation of Nazca subduction along the Andes: Nature, v. 565, p. 441–447, https://doi.org/10.1038/ s41586-018-0860-1.
- Clennett, E.J., Sigloch, K., Mihalynuk, M.G., Seton, M., Henderson, M.A., Hosseini, K., Mohammadzaheri, A., Johnston, S.T., Müller, R.D., 2020, A Quantitative Tomotectonic Plate Reconstruction of Western North America and the Eastern Pacific Basin: Geochemistry, Geophysics, Geosystems, e2020GC009117, https://doi. org/10.1029/2020GC009117.
- Coe, R.S., Globerman, B.R., Plumley, P.W., and Thrupp, G.A., 1985, Paleomagnetic results from Alaska and their tectonic implications, in Howell, D.G., ed., Tectonostratigraphic Terranes of the Circum-Pacific Region: American Association of Petroleum Geologists, Circum-Pacific Council for Energy and Mineral Resources Series, v. 1, p. 85–108.
- Cole, R.B., Nelson, S.W., Layer, P.W., and Oswald, P.J., 2006, Eocene volcanism above a depleted mantle slab window in southern Alaska: Geological Society of America Bulletin, v. 118, no. 1–2, p. 140–158, https:// doi.org/10.1130/B25658.1.
- Cowan, D.S., 2003, Revisiting the Baranof-Leech River hypothesis for early Tertiary coastwise transport of the Chugach-Prince William terrane: Earth and Planetary

- Science Letters, v. 213, no. 3, p. 463–475, https://doi.org/10.1016/S0012-821X(03)00300-5.
- Cowan, D.S., Brandon, M.T., and Garver, J.I., 1997, Geological tests of hypotheses for large coastwise displacements; a critique illustrated by the Baja British Columbia controversy: American Journal of Science, v. 297, no. 2, p. 117–173, https://doi.org/10.2475/ais.297.2.117.
- Davidson, C., and Garver, J.I., 2017, Age and origin of the Resurrection ophiolite and associated turbidites of the Chugach–Prince William Terrane, Kenai Peninsula, Alaska: The Journal of Geology, v. 125, no. 6, p. 681– 700, https://doi.org/10.1086/693926.
- Day, E.M., Pavlis, T.L., and Amato, J.M., 2016, Detrital zircon ages indicate an Early Cretaceous episode of blueschist-facies metamorphism in southern Alaska: Implications for the Mesozoic paleogeography of the northern Cordillera: Lithosphere, v. 8, no. 5, p. 451– 462, https://doi.org/10.1130/L525.1.
- Dickinson, W.R., and Snyder, W.S., 1979, Geometry of Subducted Slabs Related to San Andreas Transform: The Journal of Geology, v. 87, no. 6, p. 609–627, https://doi.org/10.1086/628456.
- Domeier, M., Shephard, G.E., Jakob, J., Gaina, C., Doubrovine, P.V., and Torsvik, T.H., 2017, Intraoceanic subduction spanned the Pacific in the Late Cretaceous–Paleocene: Science Advances, v. 3, no. 11, p. 1–5, https://doi.org/10.1126/sciadv.aao2303.
- Dziewonski, A.M., and Anderson, D.L., 1981, Preliminary reference Earth model: Physics of the Earth and Planetary Interiors, v. 25, no. 4, p. 297–356, https://doi.org/10.1016/0031-9201(81)90046-7.
- Eddy, M.P., Bowring, S.A., Umhoefer, P.J., Miller, R.B., McLean, N.M., and Donaghy, E.E., 2016, High-resolution temporal and stratigraphic record of Siletzia's accretion and triple junction migration from nonmarine sedimentary basins in central and western Washington: Geological Society of America Bulletin, v. 128, no. 3–4, p. 425–441, https://doi.org/10.1130/B31335.1.
- Eddy, M.P., Clark, K.P., and Polenz, M., 2017, Age and volcanic stratigraphy of the Eocene Siletzia oceanic plateau in Washington and on Vancouver Island: Lithosphere, v. 9, no. 4, p. 652–664, https://doi.org/10.1130/ L650.1.
- Engdahl, E., and Villasenor, A., 2002, Global seismicity: 1900–1999, in Lee, W., Kanamori, H., Jennings, P., and Kisslinger, C., eds., International Handbook of Earthquake and Engineering Seismology, Part A: International Geophysics: Cambridge, UK, Academic Press, v. 81, p. 665–690, https://doi.org/10.1016/ S0074-6142(02)80244-3.
- Engebretson, D.C., Cox, A., and Gordon, R.G., 1985, Relative motions between oceanic and continental plates in the Pacific Basin, in Engebretson, D.C., Cox, A., and Gordon, R.G., eds., Relative Motions Between Oceanic and Continental Plates in the Pacific Basin: Geological Society of America Special Paper 206, p. 1–59, https://doi.org/10.1130/SPE206-p1.
- Farris, D.W., and Paterson, S.R., 2009, Subduction of a segmented ridge along a curved continental margin: Variations between the western and eastern Sanak–Baranof belt, southern Alaska: Tectonophysics, v. 464, no. 1, p. 100–117, https://doi.org/10.1016/ j.tecto.2007.10.008.
- Finzel, E.S., and Ridgway, K.D., 2017, Links between sedimentary basin development and Pacific Basin plate kinematics recorded in Jurassic to Miocene strata on the western Alaska Peninsula: Lithosphere, v. 9, no. 1, p. 58–77, https://doi.org/10.1130/L592.1.
- Finzel, E.S., Trop, J.M., Ridgway, K.D., and Enkelmann, E., 2011, Upper plate proxies for flat-slab subduction processes in southern Alaska: Earth and Planetary Science Letters, v. 303, no. 3, p. 348–360, https://doi. org/10.1016/j.epsl.2011.01.014.
- Garver, J.I., and Davidson, C.M., 2015, Southwestern Laurentian zircons in Upper Cretaceous flysch of the Chugach-Prince William terrane in Alaska: American Journal of Science, v. 315, no. 6, p. 537–556, https:// doi.org/10.2475/06.2015.02.
- Gehrels, G., Rusmore, M., Woodsworth, G., Crawford, M., Andronicos, C., Hollister, L., Patchett, J., Ducea, M., Butler, R., Klepeis, K., Davidson, C., Friedman,

- R., Haggart, J., Mahoney, B., Crawford, W., Pearson, D., and Girardi, J., 2009, U-Th-Pb geochronology of the Coast Mountains batholith in north-coastal British Columbia: Constraints on age and tectonic evolution: Geological Society of America Bulletin, v. 121, no. 9-10, p. 1341–1361, https://doi.org/10.1130/B26404.1.
- Goes, S., Govers, R., Schwartz, S., and Furlong, K., 1997, Three-dimensional thermal modeling for the Mendocino Triple Junction area: Earth and Planetary Science Letters, v. 148, no. 1, p. 45–57, https://doi.org/10.1016/ S0012-821X(97)00044-7.
- Gou, T., Zhao, D., Huang, Z., and Wang, L., 2019, Aseismic deep slab and mantle flow beneath Alaska: Insight from anisotropic tomography: Journal of Geophysical Research. Solid Earth, v. 124, no. 2, p. 1700–1724, https://doi.org/10.1029/2018JB016639.
- Gutscher, M.-A., Maury, R., Eissen, J.-P., and Bourdon, E., 2000, Can slab melting be caused by flat subduction?: Geology, v. 28, no. 6, p. 535–538, https://doi .org/10.1130/0091-7613(2000)28<535:CSMBCB>2. 0.CO:2.
- Haeussler, P.J., Bradley, D., Goldfarb, R., Snee, L., and Taylor, C., 1995, Link between ridge subduction and gold mineralization in southern Alaska: Geology, v. 23, no. 11, p. 995–998, https://doi.org/10.1130/0091-7613(1995)023<0995:LBRSAG>2.3.CO;2.
- Haeussler, P.J., Bradley, D.C., Wells, R.E., and Miller, M.L., 2003, Life and death of the resurrection plate: Evidence for its existence and subduction in the northeastern Pacific in Paleocene-Eocene time: Geological Society of America Bulletin, v. 115, no. 7, p. 867–880, https://doi .org/10.1130/0016-7606(2003)115<0867:LADOTR>2 .0.CO;2.
- Hayes, G.P., Moore, G.L., Portner, D.E., Hearne, M., Flamme, H., Furtney, M., and Smoczyk, G.M., 2018, Slab2, a comprehensive subduction zone geometry model: Science, v. 362, no. 6410, p. 58–61, https://doi .org/10.1126/science.aat4723.
- Humphreys, E.D., Schmandt, B., Bezada, M.J., and Perry-Houts, J., 2015, Recent craton growth by slab stacking beneath Wyoming: Earth and Planetary Science Letters, v. 429, p. 170–180, https://doi.org/10.1016/j.epsl.2015.07.066.
- Ickeri, R.B., Thorkelson, D.J., Marshall, D.D., and Ullrich, T.D., 2009, Eocene adaktitic volcanism in southern British Columbia: Remelting of arc basalt above a slab window: Tectonophysics, v. 464, no. 1, p. 164–185, https:// doi.org/10.1016/j.tecto.2007.10.007.
- Jadamec, M.A., and Billen, M.I., 2010, Reconciling surface plate motions with rapid three-dimensional mantle flow around a slab edge: Nature, v. 465, no. 7296, p. 338– 341, https://doi.org/10.1038/nature09053.
- Li, C., van der Hilst, R.D., Engdahl, E.R., and Burdick, S., 2008, A new global model for P wave speed variations in Earth's mantle: Geochemistry, Geophysics, Geosystems, v. 9, no. 5, p. 353–357, https://doi .org/10.1029/2007GC001806.
- Li, Z.X., Mitchell, R.N., Spencer, C.J., Ernst, R., Pisarevsky, S., Kirscher, U., and Murphy, J.B., 2019, Decoding Earth's rhythms: Modulation of supercontinent cycles by longer superocean episodes: Precambrian Research, v. 323, p. 1–5, https://doi.org/10.1016/ j.precamres.2019.01.009.
- Liu, L., Gurnis, M., Seton, M., Saleeby, J., Müller, R.D., and Jackson, J.M., 2010, The role of oceanic plateau subduction in the Laramide orogeny: Nature Geoscience, v. 3, p. 353–357, https://doi.org/10.1038/ ngeo829.
- Madsen, J.K., Thorkelson, D.J., Friedman, R.M., and Marshall, D.D., 2006, Cenozoic to Recent plate configurations in the Pacific Basin: Ridge subduction and slab window magmatism in western North America: Geosphere, v. 2, no. 1, p. 11–34, https://doi.org/10.1130/GES00020.1.
- Matthews, K.J., Maloney, K.T., Zahirovic, S., Williams, S.E., Seton, M., and Müller, R.D., 2016, Global plate boundary evolution and kinematics since the late Paleozoic: Global and Planetary Change, v. 146, p. 226–250, https://doi.org/10.1016/j.gloplacha.2016.10.002
- Matthews, W.A., Guest, B., Coutts, D., Bain, H., and Hubbard, S., 2017, Detrital zircons from the Nanaimo basin, Vancouver Island, British Columbia: An independent

- test of Late Cretaceous to Cenozoic northward translation: Tectonics, v. 36, no. 5, p. 854–876, https://doi.org/10.1002/2017TC004531.
- McCrory, P.A., and Wilson, D.S., 2013, A kinematic model for the formation of the Siletz-Crescent forearc terrane by capture of coherent fragments of the Farallon and Resurrection plates: Tectonics, v. 32, no. 3, p. 718–736, https://doi.org/10.1002/tect.20045.
- Miller, İ.M., Brandon, M.T., and Hickey, L.J., 2006, Using leaf margin analysis to estimate the mid-Cretaceous (Albian) paleolatitude of the Baja BC block: Earth and Planetary Science Letters, v. 245, no. 1, p. 95–114, https://doi.org/10.1016/j.epsl.2006.02.022.
- O'Connell, K., 2009, Sedimentology, structural geology, and paleomagnetism of the Ghost Rocks Formation: Kodiak Islands, Alaska [M.S. thesis]: Davis, California, University of California, 112 p.
- O'Neill, C., Müller, D., and Steinberger, B., 2005, On the uncertainties in hot spot reconstructions and the significance of moving hot spot reference frames: Geochemistry, Geophysics, Geosystems, v. 6, no. 4, p. 1–35, https://doi.org/10.1029/2004GC000784.
- Pavlis, G.L., Sigloch, K., Burdick, S., Fouch, M.J., and Vernon, F.L., 2012, Unraveling the geometry of the Farallon plate: Synthesis of three-dimensional imaging results from USArray: Tectonophysics, v. 532–535, p. 82–102, https://doi.org/10.1016/j.tecto.2012.02.008.
- Pavlis, T., Amato, J., Trop, J., Ridgway, K., Roeske, S., and Gehrels, G., 2019, Subduction polarity in ancient arcs: A call to integrate geology and geophysics to decipher the Mesozoic tectonic history of the Northern Cordillera of North America: GSA Today, v. 29, no. 11, p. 4–10, https://doi.org/10.1130/GSATG402A.1.
- Plumley, P.W., Coe, R.S., and Byrne, T., 1983, Paleomagnetism of the Paleocene Ghost Rocks Formation, Prince William Terrane, Alaska: Tectonics, v. 2, no. 3, p. 295–314, https://doi.org/10.1029/TC002i003p00295.
- Ren, Y., Stutzmann, E., van der Hilst, R.D., and Besse, J., 2007, Understanding seismic heterogeneities in the lower mantle beneath the Americas from seismic tomography and plate tectonic history: Journal of Geophysical Research. Solid Earth, v. 112, no. B1.
- Richards, F.D., Hoggard, M.J., Cowton, L.R., and White, N.J., 2018, Reassessing the thermal structure of oceanic lithosphere with revised global inventories of basement depths and heat flow measurements: Journal of Geophysical Research. Solid Earth, v. 123, no. 10, p. 9136– 9161, https://doi.org/10.1029/2018JB015998.
- Russo, R.M., VanDecar, J.C., Comte, D., Moncanu, V.I., Gallego, A., and Murdie, R.E., 2010, Subduction of the Chile Ridge: Upper mantle structure and flow: GSA Today, v. 20, no. 9, p. 4–10, https://doi.org/10.1130/ GSATG61A.1.
- Saleeby, J., 2003, Segmentation of the Laramide Slab: Evidence from the southern Sierra Nevada region: Geological Society of America Bulletin, v. 115, no. 6, p. 655–668, https://doi.org/10.1130/0016-7606(2003)115<0655:SOTLSF>2.0.CO;2.
- Scharman, M.R., and Pavlis, T.L., 2012, Kinematics of the Chugach metamorphic complex, southern Alaska: Plate geometry in the north Pacific margin during the Late Cretaceous to Eocene: Tectonics, v. 31, no. 4, p. 1–14, https://doi.org/10.1029/2011TC003034.
- Schmandt, B., and Humphreys, E., 2011, Seismically imaged relict slab from the 55 Ma Siletzia accretion to the northwest United States: Geology, v. 39, no. 2, p. 175–178, https://doi.org/10.1130/G31558.1.
- Schmandt, B., and Lin, F.-C., 2014, P and S wave tomography of the mantle beneath the United States: Geophysical Research Letters, v. 41, no. 18, p. 6342–6349, https://doi.org/10.1002/2014GL061231.
- Schmid, C., Goes, S., van der Lee, S., and Giardini, D., 2002, Fate of the Cenozoic Farallon slab from a comparison of kinematic thermal modeling with tomographic images: Earth and Planetary Science Letters, v. 204, no. 1, p. 17– 32, https://doi.org/10.1016/S0012-821X(02)00985-8.
- Severinghaus, J., and Atwater, T., 1990, Cenozoic geometry and thermal state of the subducting slabs beneath western North America, in Wernicke, B.P., ed., Basin and Range Extensional Tectonics Near the Latitude of Las Vegas, Nevada: Geological Society of America Memoir 176, p. 1–22, https://doi.org/10.1130/MEM176-p1.

- Sigloch, K., 2011, Mantle provinces under North America from multifrequency P wave tomography: Geochemistry, Geophysics, Geosystems, v. 12, no. 2, p. 1–27, https://doi.org/10.1029/2010GC003421.
- Sigloch, K., and Mihalynuk, M.G., 2017, Mantle and geological evidence for a Late Jurassic–Cretaceous suture spanning North America: Geological Society of America Bulletin, v. 129, no. 11–12, p. 1489–1520, https://doi.org/10.1130/B31529.1.
- Sisson, V.B., Pavlis, T.L., Roeske, S.M., and Thorkelson, D.J., 2003a, Introduction: An overview of ridge-trench interactions in modern and ancient settings, in Sisson, V.B., Roeske, S.M., and Pavlis, T.L., eds., Geology of a Transpressional Orogen Developed During Ridgetrench Interaction Along the North Pacific Margin: Geological Society of America Special Paper 371, p. 1– 18, https://doi.org/10.1130/0-8137-2371-X.1.
- Sisson, V.B., Poole, A.R., Harris, N.R., Cooper Burner, H., Pavlis, T.L., Copeland, P., Donelick, R.A., and McLelland, W.C., 2003b, Geochemical and geochronologic constraints for genesis of a tonalite-trondhjemite suite and associated mafic intrusive rocks in the eastern Chugach Mountains, Alaska: A record of ridgetransform subduction, in Sisson, V.B., Roeske, S.M., and Pavlis, T.L., eds., Geology of a Transpressional Orogen Developed During Ridge-trench Interaction Along the North Pacific Margin: Geological Society of America Special Paper 371, p. 293–326, https://doi. org/10.1130/0-8137-2371-X.293.
- Stamatakos, J.A., Trop, J.M., and Ridgway, K.D., 2001, Late Cretaceous paleogeography of Wrangellia: Paleomagnetism of the MacColl Ridge Formation, southern Alaska, revisited: Geology, v. 29, no. 10, p. 947–950, https://doi.org/10.1130/0091-7613(2001)029<0947:LC POWP>2.0.CO;2.
- Surpless, K.D., Sickmann, Z.T., and Koplitz, T.A., 2014, East-derived strata in the Methow basin record rapid mid-Cretaceous uplift of the southern Coast Mountains batholith: Canadian Journal of Earth Sciences, v. 51, no. 4, p. 339–357, https://doi.org/10.1139/cjes-2013-0144.
- ten Brink, U.S., Miller, N.C., Andrews, B.D., Brothers, D.S., and Haeussler, P.J., 2018, Deformation of the Pacific/ North America plate boundary at Queen Charlotte Fault: The Possible role of rheology: Journal of Geophysical Research. Solid Earth, v. 123, no. 5, p. 4223–4242, https://doi.org/10.1002/2017JB014770.
- Terhune, P.J., Benowitz, J.A., Trop, J.M., O'Sullivan, P.B., Gillis, R.J., and Freymueller, J.T., 2019, Cenozoic tectono-thermal history of the southern Talkeetna Mountains, Alaska: Insights into a potentially alternating convergent and transform plate margin: Geosphere, v. 15, no. 5, p. 1539–1576, https://doi .org/10.1130/GES02008.1.
- Thorkelson, D.J., 1996, Subduction of diverging plates and the principles of slab window formation: Tectonophysics, v. 255, no. 1, p. 47–63, https://doi.org/10.1016/0040-1951(95)00106-9.
- Thorkelson, D.J., and Breitsprecher, K., 2005, Partial melting of slab window margins: Genesis of adaktic and non-adaktic magmas: Lithos, v. 79, no. 1, p. 25–41, https://doi.org/10.1016/j.lithos.2004.04.049.
- Thorkelson, D.J., and Taylor, R.P., 1989, Cordilleran slab windows: Geology, v. 17, no. 9, p. 833–836, https:// doi.org/10.1130/0091-7613(1989)017<0833:CSW>2. 3 CO:2
- Thorkelson, D.J., Madsen, J.K., and Sluggett, C.L., 2011, Mantle flow through the Northern Cordilleran slab window revealed by volcanic geochemistry: Geology, v. 39, no. 3, p. 267–270, https://doi.org/10.1130/ G31522.1.
- Torsvik, T.H., Müller, R.D., Van der Voo, R., Steinberger, B., and Gaina, C., 2008, Global plate motion frames: Toward a unified model: Reviews of Geophysics, v. 46, no. 3, p. 1–44, https://doi.org/10.1029/2007RG000227.
- Torsvik, T.H., Steinberger, B., Shephard, G.E., Doubrovine, P.V., Gaina, C., Domeier, M., Conrad, C.P., and Sager, W.W., 2019, Pacific-Panthalassic reconstructions: Overview, errata and the way forward: Geochemistry, Geophysics, Geosystems, v. 20, no. 7, p. 3659–3689, https://doi.org/10.1029/2019GC008402.
- Umhoefer, P., 2003, A model for the North America Cordillera in the Early Cretaceous: Tectonic escape related to

- arc collision of the Guerrero terrane and a change in North America plate motion, *in* Johnson, S.E., Paterson, S.R., Fletcher, J.M., Girty, G.H., Kimbrough, D.L., and Martín-Barajas, A., eds., Tectonic Evolution of Northwestern Mexico and the Southwestern USA: Geological Society of America Special Paper 374, p. 117–134, https://doi.org/10.1130/0-8137-2374-4.117
- Vaes, B., van Hinsbergen, D.J.J., and Boschman, L.M., 2019, Reconstruction of subduction and back-arc spreading in the NW Pacific and Aleutian Basin: Clues to causes of Cretaceous and Eocene plate reorganizations: Tectonics, v. 38, no. 4, p. 1367–1413, https://doi .org/10.1029/2018TC005164.
- van der Meer, D.G., van Hinsbergen, D.J.J., Spakman, W., 2018, Altlas of the underworld: Slab remnants in the mantle, their sinking history, and a new outlook on lower mantle viscosity: Tectonophysics, v. 723, p. 309– 448, https://doi.org/10.1016/j.tecto.2017.10.004.
- Wells, R., Bukry, D., Friedman, R., Pyle, D., Duncan, R., Haeussler, P.J., and Wooden, J., 2014, Geologic his-

- tory of Siletzia, a large igneous province in the Oregon and Washington Coast Range: Correlation to the geomagnetic polarity time scale and implications for a long-lived Yellowstone hotspot: Geosphere, v. 10, no. 4, p. 692–719, https://doi.org/10.1130/GES01018.1.
- Woods, M.T., and Davies, G.F., 1982, Late Cretaceous genesis of the Kula plate: Earth and Planetary Science Letters, v. 58, no. 2, p. 161–166, https://doi .org/10.1016/0012-821X(82)90191-1.
- Wu, J., and Suppe, J., 2017, Proto-South China Sea plate tectonics using subducted slab constraints from tomography: Journal of Earth Science, v. 29, p. 1304–1318.
- Wu, J., Suppe, J., Lu, R., and Kanda, R., 2016, Philippine Sea and East Asian plate tectonics since 52 Ma constrained by new subducted slab reconstruction methods: Journal of Geophysical Research. Solid Earth, v. 121, no. 6, p. 4670–4741, https://doi.org/10.1002/2016JB012923.
- Wyld, S.J., Umhoefer, P., and Wright, J., 2006, Reconstructing northern Cordilleran terranes along known Cre-

- taceous and Cenozoic strike-slip faults: Implications for the Baja British Columbia hypothesis and other models, *in* Haggart, J.W., Enkin, R.J., and Monger, J.W.H., eds., Paleogeography of the North American Cordillera: Evidence For and Against Large-scale Displacements: Geological Association of Canada Special Paper, v. 46, p. 277–298.
- Zahirovic, S., Müller, R.D., Seton, M., and Flament, N., 2015, Tectonic speed limits from plate kinematic reconstructions: Earth and Planetary Science Letters, v. 418, p. 40–52, https://doi.org/10.1016/ j.epsl.2015.02.037.

SCIENCE EDITOR: WENJIAO XIAO ASSOCIATE EDITOR: EMILY FINZEL

Manuscript Received 26 February 2020 Revised Manuscript Received 29 May 2020 Manuscript Accepted 10 August 2020

Printed in the USA